Int. J. Adv. Eng. Pure Sci. 2019, 3: 255-260
DOI: 10.7240/jeps.560040

**RESEARCH ARTICLE** / ARAŞTIRMA MAKALESİ

# Structure and Magnetic Properties $Zn_{0.96}Cu_{0.01}Ni_{0.03}O$ Nanoparticles

## $Zn_{0.96}Cu_{0.01}Ni_{0.03}O$ Nanoparçacıkların Yapısal ve Manyetik Özellikleri

**Adil GÜLER**

*Marmara University, Ataturk Faculty of Education, Department of Computer and Instructive Technology Teacher, 34722 Goztepe, Istanbul, Turkey.*

**Abstract**

$Zn_{0.96}Cu_{0.01}Ni_{0.03}O$ nanoparticles were prepared by sol-gel technique and annealed under wide temperature range (450, 500, 550, 600, 700, 800, and 900 $^0$C). To figure out the possible structural phases X-ray diffraction technique (XRD) was used. The lattice parameters were calculated by Rietveld analysis and correlated by annealing temperatures. For the synthesized nanoparticles, the optimum annealing temperatures were achieved at 450, 500, and 550 °C and further annealing temperature increment gave rise to secondary NiO peaks. The Scanning Electron Microscope (SEM) images show random ball-shaped particle distribution. Energy dispersive X-ray spectroscopy (EDX) showed only the peaks belong to the composition. Magnetic measurements were performed using Quantum Design Vibrating Sample Magnetometer (QDVSM) tool for $Zn_{0.96}Cu_{0.01}Ni_{0.03}O$ nanosystems. From the DC magnetic field dependent magnetization curves, clear paramagnetic behavior was revealed for all Cu-Ni co-doped ZnO nanoparticles.

**Keywords:** Sol-gel method, Cu, Ni, and ZnO nanosystems, Magnetic properties.

**Öz**

$Zn_{0.96}Cu_{0.01}Ni_{0.03}O$ nanoparçacıkları, sol-gel tekniği ile hazırlanıp geniş sıcaklık aralığında (450, 500, 550, 600, 700, 800, 900 ° C) tavlandı. Olası yapısal fazları belirlemek için X-ışını kırınım tekniği (XRD) kullanılmıştır. Kafes parametreleri Rietveld analizi ile hesaplanmış ve tavlama sıcaklıkları ile ilişkilendirilmiştir. Sentezlenen nanoparçacıklar için, optimum tavlama sıcaklıkları 450, 500 ve 550 ° C'de elde edildi ve ayrıca tavlama sıcaklığı artışı ikincil NiO fazlarına yol açmıştır. Taramalı Elektron Mikroskobu (SEM) görüntüleri rastgele küre şeklindeki parçacık dağılımını göstermektedir. Enerji dağıtıcı X-ışını spektroskopisi (EDX) sadece kompozisyona ait pikleri göstermektedir. $Zn_{0.96}Cu_{0.01}Ni_{0.03}O$ nanoparçacıkları için manyetik ölçümler, Kuantum Dizayn Titreşen Örnek Manyetometresi (QDVSM) kullanılarak yapıldı. DC manyetik alana bağlı mıknatıslanma eğrilerinden, tüm Cu-Ni ortak katkılı ZnO nanoparçacıklarının net paramanyetik davranışı gösterildi.

**Anahtar Kelimeler:** Sol-gel metot, Cu, Ni, ve ZnO nanosistemleri, Manyetik özellikler.

## I. Introduction

The application and the researches on Zinc oxide (ZnO) and its doped forms have an increasing interest due to offering controllable varying physical properties [1-6]. The usage of ZnO and its doped forms exhibit board range industrial applications in biomaterials, spintronics, optoelectronics, and cosmetics. ZnO and its doped forms also offer an extra opportunity with the property of adjusting size and band gap [4-12]. ZnO is in the one of the dilute magnetic semiconductor (DMS) materials' family with a wide band-gap (3.37 eV) and a large exciton binding energy (60 meV). The magnetic and the optical properties of ZnO and its doped forms strongly depends on the defects and impurities in the synthesized matrix of ZnO and to optimize the desired physical properties some certain elements especially transition metals (TM) (Fe, Co, Cu, Ni, and Mn) are needed to be introduced into ZnO. Adding TM into the ZnO matrix is also used in adjusting band gaps [3]. The reports in the literature show the significance of Ni and Cu elemental dopes into ZnO due to observing the room temperature (RT) ferromagnetism [13, 14]. Due to the property of near radius to ZnO (0.74 Å), Cupper (0.73 Å) and Nickel (0.69 Å) elements are known

**Sorumlu yazar/Corresponding Author:** Adil GÜLER, **Tel:** 0 532 765 28 66, **e-posta:** adil.guler@marmara.edu.tr
**Gönderilme/Submitted:** 02.05.2019, **Düzenleme/Revised:** 20.05.2019, **Kabul/Accepted:** 12.06.2019

both affecting magnetic properties and not to distort hexagonal Wurtzite structure [15-17]. It is known in the literature that Ni exhibits RT ferromagnetism and Cu has the property of deep level impurity [18, 19].

In this presented study, the effect of annealing temperature on structural, morphological, and the magnetic properties were revealed for $Zn_{0.96}Cu_{0.01}Ni_{0.03}O$ nanosystems and the correlations between the obtained physical results were established.

## II. Materials and Methods

Sol-gel synthesizing technique was used to obtain $Zn_{0.96}Cu_{0.01}Ni_{0.03}O$ nanoparticles annealed at a wide range from 450 to 900 °C. In the synthesizing stage, the chemicals as precursor materials, nickel acetate tetra hydrate, copper acetate tetra hydrate, and zinc acetate dehydrate. For homogenous and clear solutions, methanol and acetyl acetone were added into the final mixture. The obtained final solution was stirred at RT by means of a magnetic stirrer. The solvents in the stirred solutions were then removed and preheated at 200–350 °C for 10 min under air [1, 4]. Heat treatment was applied for each $Zn_{0.96}Cu_{0.01}Ni_{0.03}O$ sample separately using a wide temperature range (450, 500, 550, 600, 700, 800, and 900 $^0$C). To reveal the structural phases and indexes of $Zn_{0.96}Cu_{0.01}Ni_{0.03}O$ samples X-Ray diffraction measurement (Rigaku diffractometer with Cu $K_a$ radiation source) together with Rietveld analysis was provided. The morphology properties were determined for $Zn_{0.96}Cu_{0.01}Ni_{0.03}O$ nanosystems my means of JEOL, JSM-5910LV model SEM tool. The presented magnetic properties were obtained by using QDVSM tool for $Zn_{0.96}Cu_{0.01}Ni_{0.03}O$ nanosystems.

## III. Results and discussions

To reveal the possible phases XRD studies were performed and exhibited in Fig. 1 (a), (b), and (c) for $Zn_{0.96}Cu_{0.01}Ni_{0.03}O$ nanosystems. As seen in Fig. 1 (a) the measurement was taken between 20° and 80° region and the maximum peak was indexed as (101) almost at the position of Θ=36.693°. The samples annealed at different temperatures depicted almost the same XRD pattern with a small ignorable NiO peak revealed at Θ=43.061° and the rest of the peaks belong to the pure ZnO peaks with the space group of P63mc. To figure out the possible peak shifts and together with structural distortion in $Zn_{0.96}Cu_{0.01}Ni_{0.03}O$ samples, Fig. 1 (b) was presented and figured out that except for the sample annealed at 450 °C, the peak position are at the same 2 Θ angle position and the shift in the sample annealed at 450 °C is almost 0.02° which is small enough to be ignored. These results were also confirmed by c/a rates which are almost 1.6 for all samples. As given in Table 1. Rietveld refinement was provided by means of GSAS program for the sample annealed at 700 °C to clarify the possible phases and lattice parameters in Fig. 1 (c). As shown in Fig. 1 (c), the difference patterns' peaks given by blue colour is small enough and the observed (black colour) and the calculated (red colour) peaks match well with the other peaks. This result is an indication of the well-prepared and refined sample.

**Table 1.** Average particle size, cell volumes, c/a rates, and lattice parameters.

| *Temperature (°C)* | *D (nm)* | *a(Å)* | *c(Å)* | *c/a* | *Volume, V (Å$^3$)* |
|---|---|---|---|---|---|
| 450 | 22.894 | 3.242 | 5.198 | 1.603 | 54.634 |
| 500 | 23.522 | 3.248 | 5.205 | 1.602 | 54.910 |
| 550 | 24.133 | 3.244 | 5.213 | 1.607 | 54.860 |
| 600 | 24.758 | 3.250 | 5.207 | 1.602 | 54.998 |
| 700 | 24.864 | 3.249 | 5.202 | 1.601 | 54.912 |
| 800 | 26.891 | 3.247 | 5.203 | 1.602 | 54.890 |
| 900 | 28.182 | 3.241 | 5.187 | 1.600 | 54.484 |

The temperature-dependent particle size, lattice parameters, c/a rates, and cell volume variations were demonstrated in Table 1. As seen in Table 1 and Fig. 2, while the maximum value was obtained at 600 °C annealing temperature for in-plane lattice parameter, out of plane lattice parameter c and the cell volume V values exhibited the maximum at 550 °C annealing temperature. After the reached maximums, c, a, and V parameters showed a decrement with increasing annealing temperature. The decrement in V values might be an indication of increasing chemical pressure in the unit cell. The average particle size (D) in Table 1 was calculated by Debye-Sherrer formula:

$$D = \frac{K\lambda}{\beta Cos\theta} \quad (1)$$

Where 0.9 and 0.15406 nm are the constants attributed to K and X-ray wavelength l, b is the intensity of the full width at the half-maximum (FWHM) at the q position, and the Bragg diffraction angle is q. The average particle size variations due to annealing temperature were exhibited in Table 1.

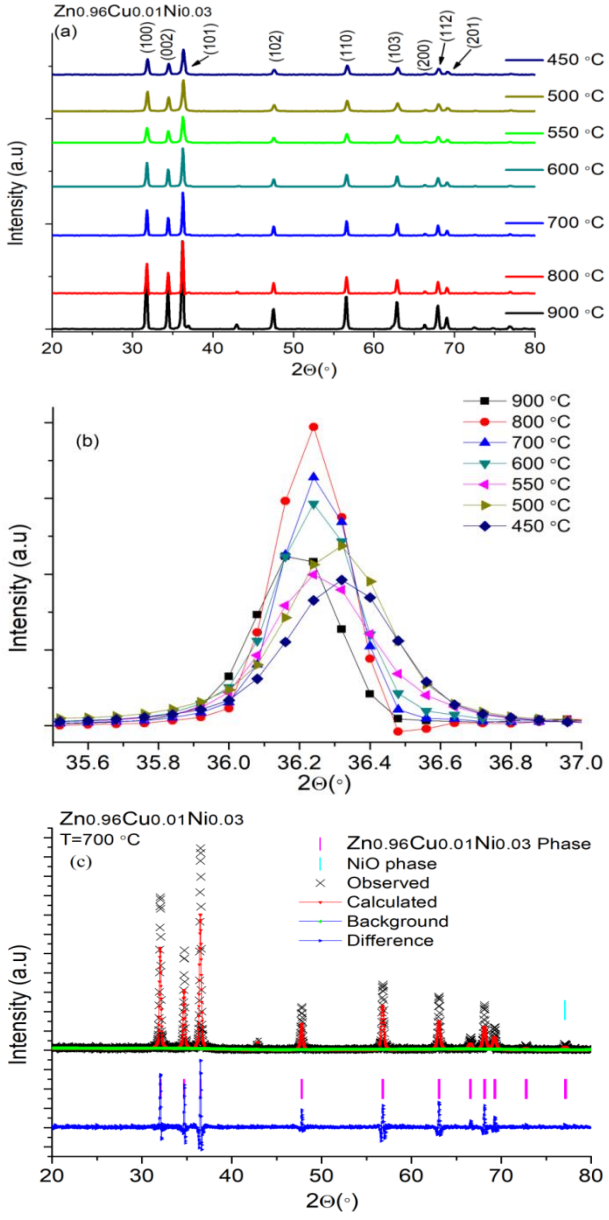


**Fig 1.** X-ray diffraction of $Zn_{0.96}Cu_{0.01}Ni_{0.03}O$ samples in (a), the demonstration of the peak positions in (b), and Rietveld analysis of $Zn_{0.96}Cu_{0.01}Ni_{0.03}O$ sample annealed at 700 °C in (c).

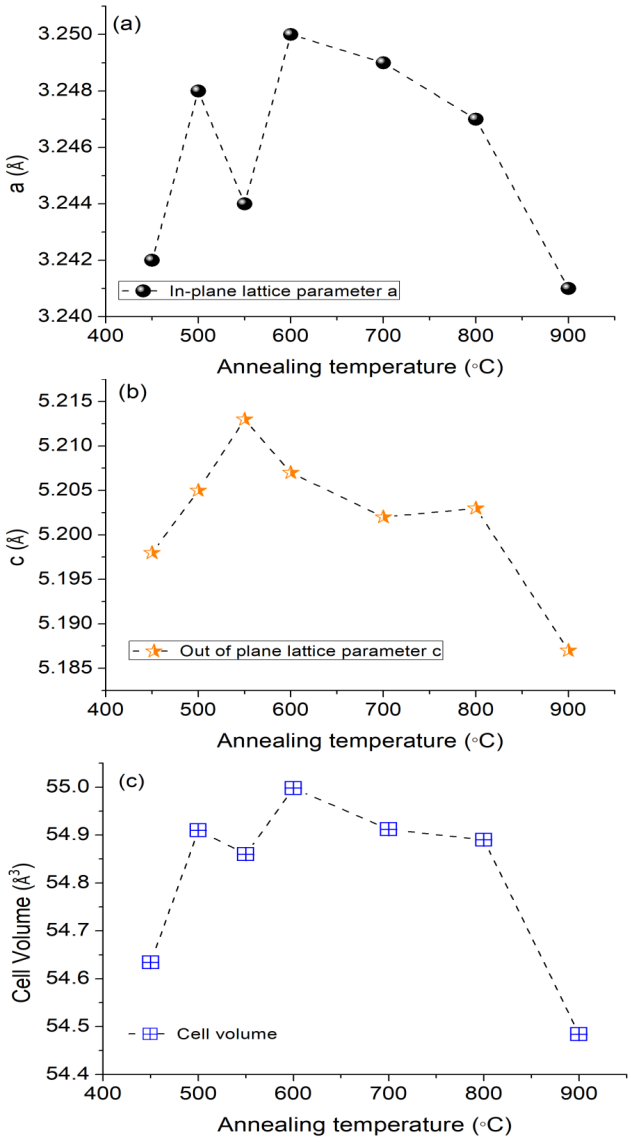


**Fig 2.** The variation of annealing temperature-dependent a and c lattice parameters and cell volume variations for $Zn_{0.96}Cu_{0.01}Ni_{0.03}O$ samples in (a), (b), and (c) respectively.

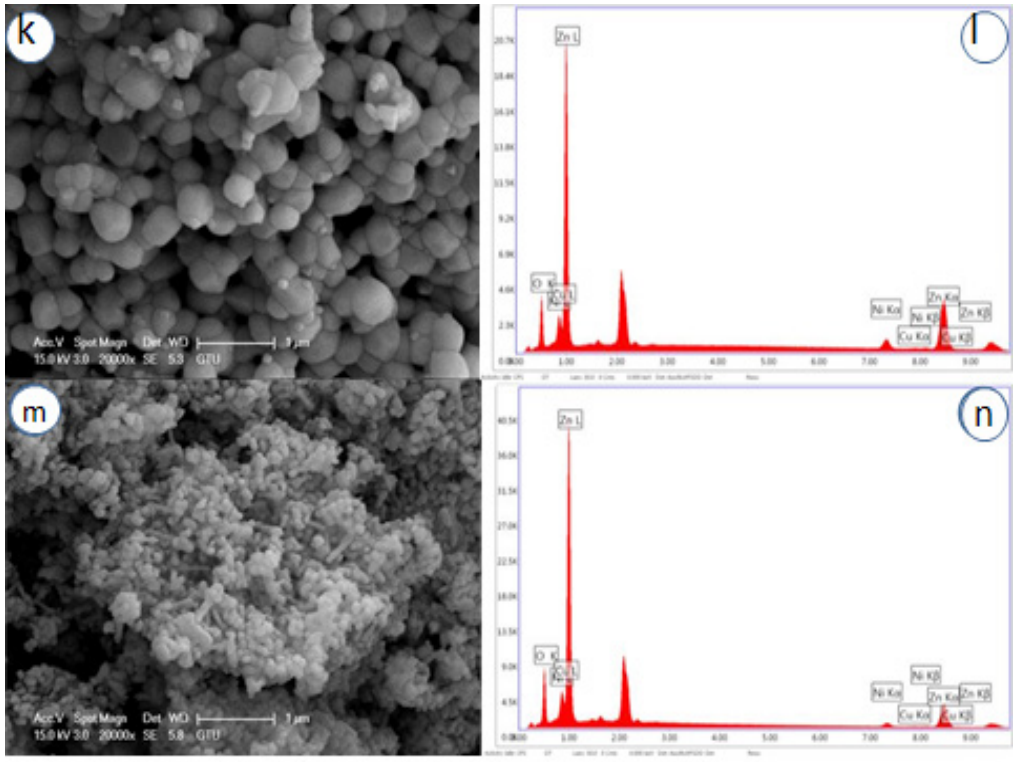


**Fig 3.** SEM images in (a), (c), (e), (g),(k), and (m) and EDX figures in (b), (d), (f), (h),(I), and (n) for $Zn_{0.96}Cu_{0.01}Ni_{0.03}O$ samples.

To figure out the particle distribution, SEM study was performed for $Zn_{0.96}Cu_{0.01}Ni_{0.03}O$ samples annealed at 500, 550, 600, 700, 800, and 900 °C which was demonstrated in Fig. 3 (a), (c), (e), (g), (k), and (m) respectively. All SEM images were presented in 1 μm magnifications. As seen in all SEM images in Fig. 3, cluster type random particle agglomeration is dominant with spherical type particle shapes. The elemental compositions of the $Zn_{0.96}Cu_{0.01}Ni_{0.03}O$ nanosystems annealed at varying temperatures were provided by EDX measurements in Fig. 3 (b), (d), (f), (h), (l), and (n). All peaks belonged to the Zn, Ni, Cu, and O elements and no other elemental contribution was detected in EDX measurements. The desired stoichiometry was provided for $Zn_{0.96}Cu_{0.01}Ni_{0.03}O$ samples and presented in Table 2.

**Table 2.** The atomic percentages of all $Zn_{0.96}Cu_{0.01}Ni_{0.03}O$ nanoparticles provided by EDX system.

| $Zn_{0.96}Cu_{0.01}Ni_{0.03}O$ | Elements and Atomic Ratios (%) | | | |
|---|---|---|---|---|
| Annealling Temp. (°C) | ZnK | CuK | NiK | OK |
| 500 | 74.42 | 4.59 | 2.38 | 18.61 |
| 550 | 73.89 | 3.43 | 2.71 | 19.97 |
| 600 | 74.02 | 3.89 | 2.67 | 19.42 |
| 700 | 71.50 | 5.54 | 2.99 | 19.97 |
| 800 | 72.57 | 4.32 | 3.08 | 20.03 |
| 900 | 70.91 | 2.57 | 7.81 | 18.71 |

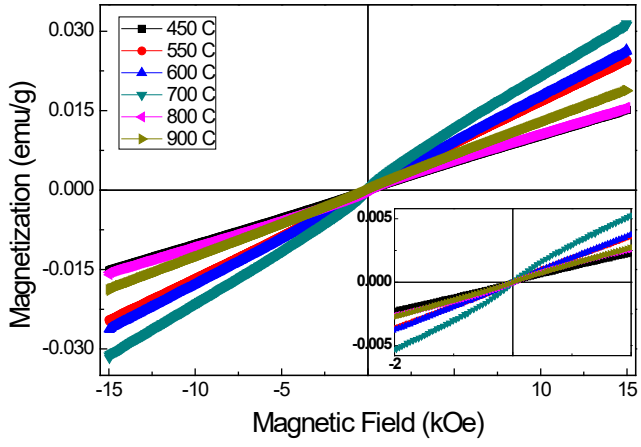


**Fig 4.** M-H curves at 300 K for $Zn_{0.96}Cu_{0.01}Ni_{0.03}O$ samples annealed at different temperatures.

According to the literature, the magnetic properties of any system greatly depend on doping elements and synthesis methods [19, 20]. The DC magnetic field-dependent magnetization curves (M vs. H) exhibited a clear paramagnetic behavior for all Cu-Ni co-doped ZnO nanoparticles. ZnO is diamagnetic, Copper is non-magnetic and it can generate

ferromagnetism in ZnO [21]. Otherwise, it is also known that the magnetic properties of NiO nanoparticles are very sensitive to size, crystal structure, and morphology [22]. For instance, the bulk NiO was found antiferromagnetic [23] but pure and Fe doped NiO nanoparticles and NiO nanotube were found ferromagnetic [22]. The origin of paramagnetism in Ni-Cu doped ZnO has a number of possibilities which are the oxygen vacancies, impurities, and zinc interstitial in the crystal structure. Actually, the main source of the paramagnetic curve in this system is the paramagnetic ZnO [24].

**Table 3.** Annealing temperature-dependent magnetic parameter variations.

| Magnetic parameters | Annealing Temperature ($^0$C) | | | | | |
|---|---|---|---|---|---|---|
| | 450 | 550 | 600 | 700 | 800 | 900 |
| Saturation Magnetization (emu/g) | 0.0154 | 0.025 | 0.027 | 0.032 | 0.016 | 0.018 |
| Remanent Magnetization (emu/g) | $1.3*10^{-5}$ | $0.7*10^{-5}$ | $5*10^{-5}$ | $4.5*10^{-5}$ | $1.8*10^{-5}$ | $1.25*10^{-5}$ |
| CoercivityField (Oe) | 8 | 3 | 20 | 11 | 7 | 3 |

Magnetic properties of samples were demonstrated in Table 3. The samples cannot reach saturation even in the presence of 15 kOe magnetic field. It is obvious that the highest magnetization value is observed in the case of 700 $^0$C annealing temperature. While the saturation magnetization value is changing between 0.57-0.052 emu/g. As can be seen in Table 3, there is no correlation variation between saturation magnetization, remanent magnetization and coercivity field with annealing temperature.

## Conclusion

$Zn_{0.96}Cu_{0.01}Ni_{0.03}O$ nanoparticles were synthesized in nanoparticle form by sol-gel technique and annealed at a wide temperature range (450, 500, 550, 600, 700, and 900 °C). While there was no trace of secondary peaks in $Zn_{0.96}Cu_{0.01}Ni_{0.03}O$ nanoparticles annealed at 450, 500, and 550°C, we observed ignorable secondary NiO peaks further increasing the annealing temperatures. From the light of this result, we figured out that up to 550 °C there is an optimum annealing temperature for $Zn_{0.96}Cu_{0.01}Ni_{0.03}O$ nanoparticles. In and out of plane lattice parameters were calculated using Rietveld refinement and c/a rate showed that there was no structural deformation because of annealing effect. In all frames of SEM images, we observed random cluster shape particle distributions. The EDX results emphasized that the desired stoichiometry was achieved and all peaks in the EDX frames belonged to $Zn_{0.96}Cu_{0.01}Ni_{0.03}O$ samples. A clear paramagnetic behavior was observed for all Cu-Ni co-doped ZnO nanoparticles from the DC magnetic field dependent magnetization curves (M vs. H). The origin of paramagnetism in Ni-Cu doped ZnO has a number of possibilities which are the oxygen vacancies, impurities, and zinc interstitial in the crystal structure.

## References


[1] Boyraz, C., Doğan, N. Arda, L. (2017). Microstructure and magnetic behavior of (Mg/Ni) co-doped ZnO nanoparticles. *Ceramics International*. 43, 15986-15991.

[2] Korbecka, A. Majewski, J. A. (2009). Nickel Sub-lattice Effects on the Optical Properties of ZnO Nanocrystals. *Low Temp. Phys*. 35(53), 28-32.

[3] Arda, L. Dogan, N. Boyraz, C. (2018). Effects of Annealing Temperature on Microstructure and Magnetic Properties of $Ni_{0.05}Zn_{0.95}Fe_2O_4$ Nanoparticles. *J. Supercond. Nov. Mag.* 31(2), 365-371.

[4] Prater, J. T. Ramachandran, S. Tiwari, A. Narayan, J. J. (2006). Co-doped ZnO dilute magnetic magnetic semiconductor. *Electron. Mater.* 35, 852.

[5] Boyraz, C. Yesilbas, B. Arda, L. (2017). The temperature effect on structural and magnetic properties of $Zn_{0.95}Fe_{0.05}O$ nanoparticles. *Journ. of Supercon. Nov. Mag*. 30(6), 1691–1698.

[6] Karmakar, D. Mandal, S. K. Kadam, R. M. Paulose, P. L. Rajarajan, A. K. Nath, T. K. Das, A. K. Dasgupta, I. Das, G. P. (2007). Ferromagnetism in Fe-doped ZnO nanocrystals: Experiment and theory. *Phys. Rev. B*. 75, 144404.

[7] Senol, S. D. Boyraz, C. Ozugurlu, E. Gungor, A. Arda, L. (2019). Band Gap Engineering of Mg Doped ZnO Nanorods Prepared by a Hydrothermal Method. *Crystal Research and Technology.* 54 (3), 1800233.

[8] Dorpe, P. V. Motsnyi, V. F. Nijboer, M. Goovaerts, E. Safarov, V. I. Das, J. Das et al. (2003). Highly efficient room temperature spin injection in a metal-insulator-semiconductor light emitting diode. *Jpn. J. Appl. Phys.* 42(5B) 502 – L504.

[9] Guler, A. Arda, L Dogan, N Boyraz, C Ozugurlu, E. (2019). The annealing effect on microstructure and ESR properties of (Cu/Ni) co-doped ZnO nanoparticles. *Ceramics International*. 45(2), 1737-1745.

[10] Goano, M. Bertazzi, F. Penna, M. Bellotti, E. (2007). Electronic structure of wurtzite ZnO: Nonlocal pseudopotential and *ab initio* calculations. *Journal of Applied Physics.* 102, 083709.

[11] Senol, S. D. Guler, A. Boyraz, C. Arda, L. (2019). Preparation Structure and Magnetic Properties of Mn-Doped ZnO Nanoparticles Prepared by Hydrothermal Method. *Journal of Superconductivity and Novel Magnetism*. DOI: 10.1007/s10948.019.5030-7.

[12] Guler, A. Tosun, M. Gungor, A. Boyraz, C. Arda, L. (2019). Effect of Annealing Temperature on Structure and Magnetic Properties of $Zn_{0.94}Mg_{0.01}Mn_{0.05}O$ Nanoparticles. *Journal of Superconductivity and Novel Magnetism*. DOI: 10.1007/s10948.019.5024-5.

[13] Venkatesan, M. Fizgerald, C. B. Lunney, J. G. J. M. Coey, D. (2004). Anisotropic Ferromagnetism in Substituted Zinc Oxide. *Phys. Rev. Lett.* 93, 177206.

[14] Liu, X. X. Lin, F. T. Sun, L. L. Cheng, W. J. Ma, X. M. Shi, W. Z. (2206). Doping concentration dependence of room-temperature ferromagnetism for Ni-doped ZnO thin films prepared by pulsed-laser deposition. *Appl. Phys. Lett*. 88, 062508.

[15] Cheng, C. W. Xu, G. Y. Zhang, H. Luo, Q. Y. (2008). Hydrothermal synthesis Ni-doped ZnO nanorods with room-temperature ferromagnetism. *Mater. Lett.* 62, 1617.

[16] Wu, D. W. Yang, M. Z. Huang, B. G. Yin, F. Liao, X. M. Y Kang,. Q. X. Chen, F. Wang, H. (2009). Preparation and properties of Ni-doped ZnO rod arrays from aqueous solution. *J. Colloid Interface Sci*. 330, 380.

[17] Ghosh, S. Srivastava, P. Pandey, B. Saurav, M. Bharadwaj, P. Avasthi, D. K. Kabiraj, D. Shivaprasad, S. M. (2008). Study of ZnO and Ni-doped ZnO synthesized by atom beam sputtering technique. *Appl. Phys. A*. 90**,** 765.

[18] Arda, L. Açıkgöz, M. Doğan, N. Akcan, D. Çakıroğlu, O. (2014). Synthesis, characaterization and ESR studies of $Zn_{1-x}Co_x$ O nanoparticles**.** ***J. Supercond Nov Magn.*** 27, 799-804.

[19] Tang, G. Shi, X. Huo, C. Wang, Z. (2013). Room temperature ferromagnetism in hydrothermally grown Ni and Cu co-doped ZnO nanorods. *Ceramics International*. 39, 4825-4829.

[20] Zhu, M. Zhang, Z. Zhong, M. Tariq, M. Li, Y. Li, W. Jin, H. Skotnicova, K. Li, Y. (2017). Oxygen vacancy induced ferromagnetism in Cu-doped ZnO. *Ceramics International*. 43(3), 3166-3170.

[21] Srinivasan, G. Seehra, M. S. (1984). Magnetic susceptibilities, their temperature variation, and exchange constants of NiO. *Physica Review B*. 29, 6295-6298.

[22] Ponnusamy, P. M. Agilan, S. Muthukumarasamy, N. Senthil, T. S. Rajesh, G. M. Venkatraman, R. Velauthapillai, D. (2016). Structural, optical and magnetic properties of undoped NiO and Fe-doped NiO nanoparticles synthesized by wet-chemical process. *Materials Characterization*. 114, 166-171.

[23] Tadic, M. Nikolic, D. Patjan, M. Blake, G. R. (2015). Magnetic properties of NiO (nickel oxide) nanoparticles. *Journal of Alloys and Compounds*. 647, 1061-1068.

[24] Dinesha, M. L. Jayanna, H. S. Ashoka, S. Chandrappa, G. T. (2009). Effect of Fe doping concentration on electrical and magnetic properties of ZnO nanoparticles prepared by solution combustion method. *Journal of Optoelectronics and Advanced Materials*.11, 964-969.